Neuroscience 291 (2015) 216–229

MOTOR NEURONS WITH DIFFERENTIAL VULNERABILITY TO DEGENERATION SHOW DISTINCT PROTEIN SIGNATURES IN HEALTH AND ALS

L. COMLEY,[a†] I. ALLODI,[a†] S. NICHTERWITZ,[a†] M. NIZZARDO,[b] C. SIMONE,[b] S. CORTI[b] AND E. HEDLUND[a*]

[a] *Department of Neuroscience, Karolinska Institutet, Retzius v. 8, 171 77 Stockholm, Sweden*

[b] *Dino Ferrari Center, Neuroscience Section, Department of Pathophysiology and Transplantation, University of Milan, Neurology Unit, Istituto Di Ricovero e Cura a Carattere Scientifico Foundation Ca' Granda Ospedale Maggiore Policlinico, Milan 20122, Italy*

Abstract—The lethal disease amyotrophic lateral sclerosis (ALS) is characterized by the loss of somatic motor neurons. However, not all motor neurons are equally vulnerable to disease; certain groups are spared, including those in the oculomotor nucleus controlling eye movement. The reasons for this differential vulnerability remain unknown. Here we have identified a protein signature for resistant oculomotor motor neurons and vulnerable hypoglossal and spinal motor neurons in mouse and man and in health and ALS with the aim of understanding motor neuron resistance. Several proteins with implications for motor neuron resistance, including $GABA_A$ receptor α1, guanylate cyclase soluble subunit alpha-3 and parvalbumin were persistently expressed in oculomotor neurons in man and mouse. Vulnerable motor neurons displayed higher protein levels of dynein, peripherin and $GABA_A$ receptor α2, which play roles in retrograde transport and excitability, respectively. These were dynamically regulated during disease and thus could place motor neurons at an increased risk. From our analysis is it evident that oculomotor motor neurons have a distinct protein signature compared to vulnerable motor neurons in brain stem and spinal cord, which could in part explain their resistance to degeneration in ALS. Our comparison of human and mouse shows the relative conservation of signals across species and infers that transgenic $SOD1^{G93A}$ mice could be used to predict mechanisms of neuronal vulnerability in man.

Key words: oculomotor, motor neuron, amyotrophic lateral sclerosis, neurodegeneration, selective vulnerability.

INTRODUCTION

Amyotrophic lateral sclerosis (ALS) is a fatal disease characterized by a progressive loss of somatic motor neurons in the spinal cord and brain stem. However, certain groups of somatic motor neurons, including those in the oculomotor nucleus (CNIII), which control eye movements, and those in Onuf's nucleus, that control pelvic muscles, are generally spared (Gizzi et al., 1992; Kubota et al., 2000; Nimchinsky et al., 2000; Haenggeli and Kato, 2002; Tjust et al., 2012). The reasons for this differential vulnerability among motor neurons remain unknown.

ALS can be inherited (familial, fALS, ∼10%) due to mutations identified in a number of genes, the two most common of which are superoxide dismutase 1 (SOD1) and C9ORF72 (chromosome 9 open reading frame 72) (Al-Chalabi et al., 2012), but the majority of ALS cases appear sporadic (sALS, ∼90%). The pathology and pattern of selective motor neuron vulnerability is similar in fALS and sALS (Shaw et al., 1997). This indicates that differential vulnerability is independent of the cause of disease. Therefore elucidation of the mechanisms of selective vulnerability in mouse models of fALS could be applicable also to sALS. Importantly, *in vivo* and *in vitro* models of fALS indicate that factors intrinsic to motor neurons are crucial for initiation of degeneration (Boillee et al., 2006; Jaarsma et al., 2008; Huang et al., 2012; Kiskinis et al., 2014), while astrocytes and microglia drive disease progression (Boillee et al., 2006; Yamanaka et al., 2008; Das and Svendsen, 2014). It therefore seems that differential expression of factors intrinsic to motor neurons render these cells more or less vulnerable to toxic events (Saxena et al., 2009; Hedlund et al., 2010; Kaplan et al., 2014). Thus, identification of cell intrinsic mechanisms of protection and vulnerability may lead to therapies preventing the progressive loss of motor neurons. Toward this goal, we previously analyzed the global gene expression profiles of vulnerable spinal and hypoglossal motor neurons and spared oculomotor and trochlear neuron groups in the normal rat and identified multiple intrinsic factors that may underlie their differential vulnerability (Hedlund et al., 2010).

To further our understanding of motor neuron vulnerability and resistance, we selected six genes that

*Corresponding author. Tel: +46-852487884.
E-mail address: eva.hedlund@ki.se (E. Hedlund).
† These authors contributed equally to this work.

Abbreviations: ALS, amyotrophic lateral sclerosis; ANOVA, analysis of variance; ChAT, choline acetyltransferase; CNIII, oculomotor nucleus; CNXII, hypoglossal nucleus; Gabra1, $GABA_A$ receptor α1; Gabra2, $GABA_A$ receptor α2; Gucy1a3, guanylate cyclase soluble subunit alpha-3; NBB, Netherlands Brain Bank; ND, non-demented; NDRI, National Disease Research Interchange; PBS, phosphate-buffered saline; PFA, paraformaldehyde; SC, spinal cord; SOD1, super oxide dismutase 1.

http://dx.doi.org/10.1016/j.neuroscience.2015.02.013
0306-4522/

Table 1. Candidate genes selected for across species analysis in health and ALS based on differential mRNA expression

Gene name	Known biological functions	Motor neurons with highest mRNA level*
		Control rat
Gucy1a3	Main receptor for nitric oxide (Zabel et al., 1998), potentially implicated in modulating Fas ligand activation (Hedlund et al., 2010)	CNIII
Parvalbumin	Calcium-binding protein with motor neuron protective effects (Van Den Bosch et al., 2002; Dekkers et al., 2004)	CNIII
Gabra1	Inhibitory synaptic transmission, neuronal excitability (Lorenzo et al., 2006; Brockington et al., 2013)	CNIII
Gabra2	Inhibitory synaptic transmission, neuronal excitability (Lorenzo et al., 2006; Brockington et al., 2013)	SC
Peripherin	Intermediate neurofilament, over-expression of which causes ALS-like MN loss (Beaulieu et al., 1999)	CNXII and SC
Dynein	Retrograde transport protein, mutations in which are linked to motor neuron degeneration (LaMonte et al., 2002; Hafezparast et al., 2003)	CNXII and SC

CNIII = oculomotor nucleus, CNXII = hypoglossal nucleus, SC = spinal cord.
* Based on our previously published gene array study (Hedlund et al., 2010).

differed in their mRNA expression between resistant and susceptible motor neurons in the healthy rodent (Hedlund et al., 2010), and analyzed the corresponding protein levels in health and ALS, in man and mouse. Specifically, the proteins analyzed in this study were guanylate cyclase soluble subunit alpha-3 (Gucy1a3), parvalbumin, $GABA_A$ receptor α1 (Gabra1), $GABA_A$ receptor α2 (Gabra2), peripherin and dynein, which all have previous implications for motor neuron disease (summarized in Table 1). Our initial analysis was performed in early symptomatic mutant $SOD1^{G93A}$ fALS mice and wild-type litter-mates. In order to elucidate if genes showed similar expression patterns and regulation in human disease and thus could be inferred to play a role in protection and vulnerability we subsequently analyzed post mortem tissues from non-demented (ND) controls and sporadic ALS patients. Our analysis showed that resistant oculomotor motor neurons have a distinct protein signature, which is relatively conserved between man and mouse. This unique profile could in part explain their preservation in ALS when other motor neurons degenerate.

EXPERIMENTAL PROCEDURES

Ethics statement

All the work involving animal or human subjects/tissues has been carried out in accordance with the Code of Ethics of the World Medical Association (Declaration of Helsinki) and with national legislation as well as our institutional guidelines. Ethical approval for the use of the human samples analyzed in this publication was obtained by Dr. Hedlund from the regional ethical review board in Stockholm, Sweden (Regionala Etikprövningsnämnden, Stockholm, EPN, http://www.epn.se/sv/stockholm/om-naemnden/), approval number 2012/111-31/1. All human tissues were obtained from the Netherlands Brain Bank (NBB, www.brainbank.nl) or the National Disease Research Interchange (NDRI, www.ndriresource.org) with the written informed consent from the donors or the next of kin. All procedures involving animals were approved by the Swedish animal ethics review board (Stockholms Norra Djurförsöksetiska nämnd, http://www.jordbruksverket.se/amnesomraden/djur/olikaslagsdjur/forsoksdjur/etiskprovning.html) with ethical approval numbers N352/11, N264/12 and N82/13 (Hedlund).

Mouse tissue processing

Analysis was performed on tissues from 112-day-old (P112) early-symptomatic $SOD1^{G93A}$ fALS mice, which display hindlimb tremors and partial denervation of motor end-plates (Fischer et al., 2004; Schaefer et al., 2005). P112 $SOD1^{G93A}$ mice on a C57Bl/6J background (Gurney, 1994) and age-matched wild-type litter-mates from the same colony, were anesthetized with avertin (tribromoethanol, Sigma) and perfused intracardially with phosphate-buffered saline (PBS) followed by 4% paraformaldehyde (PFA). Brains and spinal cords were dissected and postfixed (for 3 and 1 h respectively). All tissues were cryoprotected in sucrose and sectioned (30 μm).

Immunofluorescence analysis of mouse tissues

Tissues were blocked in 10% donkey serum (Jackson Laboratories, West Grove, PA, USA) and 0.1% Triton-X100 (Sigma-Aldrich AB, Stockholm, Sweden) in PBS for 1 h prior to incubation with primary antibodies (Table 2) overnight at 4 °C. This was followed by incubation with Alexafluor secondary antibodies (1:500) for 1 h, counter staining with either Hoechst 33342 or Neurotrace 435 (1:200, Invitrogen) and coverslipping for confocal analysis (Zeiss lsm700). Negative controls were performed for all stainings by omitting either primary or secondary antibodies.

Human tissue processing

Human brain and spinal cord tissues from ALS patients and ND controls were retrieved from the Netherlands Brain Bank (NBB, http://www.brainbank.nl) and the National Disease Research Interchange (NDRI, http://

Table 2. Antibodies used for immunofluorescence and immunohistochemistry

Target	Source	Host species	Concentration in mouse tissue	Concentration in human tissue
ChAT	Millipore	Goat	1:300	1:50
ChAT	Millipore	Rabbit	1:200	–
Dynein	Abcam	Rabbit	1:100	1:100
Gabra1	Millipore	Rabbit	1:200	1:100
Gabra2	Abcam	Rabbit	1:500	1:100
Gabra2	Santa Cruz	Goat	–	1:50
Gucy1a3	Abgent	Rabbit	–	1:60
Gucy1a3	Abcam	Rabbit	1:1000	
Parvalbumin	Millipore	Rabbit	1:500	1:200
Peripherin	Millipore	Rabbit	1:100	–
Peripherin	Millipore	Mouse	–	1:100

Table 3. Characteristics of non-demented and ALS clinical cases used for immunohistochemical analysis

Case number	Sex	Age at death	Neurological diagnosis	Postmortem delay time (h:min)	Source
1	F	58	Non-demented	14:10	NDRI
2	M	70	Non-demented	4:50	NDRI
3	F	71	Non-demented	7:10	NBB
4	M	71	Non-demented	7:40	NBB
5	F	87	Non-demented	5:00	NBB
6	F	49	ALS	3:45	NBB
7	M	65	ALS	10:30	NDRI
8	M	71	ALS	6:45	NBB
9	M	74	ALS	7:20	NDRI

NBB – Netherlands Brain Bank (http://www.brainbank.nl).
NDRI – National Disease Research Interchange (http://www.ndriresource.org/).

www.ndriresource.org/) (Ethical Approval Dnr 2012/111-31/1, Hedlund). The characteristics of ND and ALS clinical cases used for immunohistochemical analysis are listed in Table 3. Tissues from NBB were received embedded in paraffin and were sectioned (10 μm) on a sliding microtome. Tissues from NDRI were fixed in PFA, sequentially placed through sucrose gradients (2%, 10%, 20% and 30%) for cryoprotection and sectioned (40 μm) on a freezing microtome. NBB tissue was deparaffinized and all tissue was subjected to antigen retrieval (0.01 M citric acid buffer, pH 6.0 for 20 min at 95 °C) and blocking of endogenous peroxidases (3% H_2O_2 in 50% methanol in PBS) prior to staining.

Immunohistochemistry of human tissues

As the majority of the human tissues were paraffin embedded, resulting in high background levels when subjected to immunofluorescent staining, we chose to perform the analysis of human tissues with a peroxidase-based system. Tissue was blocked and incubated with primary antibodies (Table 2) as described above prior to incubation with biotinylated secondary antibodies (1:300; Jackson Laboratories) for 3 h, followed by incubation in streptavidin–biotin complex (Vectastain ABC kit Elite, Vector Laboratories, Burlingame, CA, USA) for 1 h and visualized by incubation in 3,3′-diaminobenzidine solution (DAB, Vector Laboratories). Nuclei were counterstained using Myers hematoxylin (Histolab) and tissue was dehydrated by sequential steps in increasing ethanol concentration and coverslipped using Mountex (Histolab). Brightfield images were captured using a Zeiss Axio Imager M1 Upright microscope. Negative controls were performed for all stainings by omitting either primary or secondary antibodies.

Intensity measurements

In order to assess signal intensity of candidate proteins in brain stem and spinal cord motor neurons, micrographs were taken of our regions of interest; CNIII, trochlear nucleus (CNIV), hypoglossal nucleus (CNXII) and ventral horn of the spinal cord. Acquisition settings were optimized for each candidate protein to avoid any saturation of signal, which could affect intensity calculations (Waters, 2009). Care was taken to consistently image the motor neuron population of interest at the same point on the rostral-caudal axis using morphological landmarks from atlases of rodent and human brainstem anatomy. Signal intensity of candidate proteins in motor neurons in the brain stem and spinal cord was measured by outlining individual motor neuron somas on micrographs and calculating average pixel intensity using ImageJ software (http://rsb.info.nih.gov/ij/). To aid mouse tissue analysis, sections were counter stained with Nissl (Neurotrace 435) and antibodies against choline acetyltransferase (ChAT), allowing us to easily identify motor neurons. In order to avoid bias against motor neurons with low levels of candidate protein expression all motor neurons (identified by ChAT staining) within the focal plane of a confocal micrograph (identified by a clear nucleus within the soma, stained with Nissl) were included in the analysis. In order to exclude interneurons (which also express ChAT) only cell somas with an area $\geqslant 200\ \mu m^2$ were included. To aid human tissue analysis, sections were initially stained with Nissl to identify CNIII, CNXII and ventral horn of the spinal cord. Sections were subsequently stained with antibodies against ChAT, allowing us to easily visualize motor neurons, and adjacent sections were stained and quantified for intensity levels of candidate proteins. As with rodent tissues, all motor neurons within the focal plane of a micrograph were included in the analysis. In order to exclude interneurons from our analysis of human material, only cell somas with an area $\geqslant 300\ \mu m^2$ were included.

To correct for background in images, three background intensity readings were taken per image. These readings were subsequently averaged and subtracted from the signal intensity within motor neurons of the same area to give an accurate reading of the candidate protein staining intensity. The signal

intensity of candidate proteins within CNIII was normalized to a value of one. Signal intensity of candidate proteins within CNXII and spinal cord was then compared to this value to assess if the intensity was higher or lower than that seen in CNIII. The scientists performing the intensity measurements and quantification of signal intensity for this study were blinded to the genotype of the animals and the diagnosis of the patients.

Statistical analysis

All statistical analyses were performed with GraphPad Prism software. A one-way analysis of variance (ANOVA) was used to compare the mean intensity of candidate proteins in CNIII, CNXII and spinal cord. A two-way ANOVA was used when several variables were taken into account (intensity across anatomical regions and disease status), followed by Tukey's post hoc analysis of mean differences between groups. Individual statistical tests are detailed in the figure legends. In the figures, the significance of the statistical analysis is marked by *, where $^{*}P < 0.05$, $^{**}P < 0.01$, $^{***}P < 0.001$ and $^{****}P < 0.0001$. The F value used for 2-way ANOVAs refers to the effect of genotype (wild-type versus SOD1^{G93A}). The number of animals used for each experiment is listed in the figure legends and the number of motor neurons measured for each candidate protein is listed in Table 4. All experiments for Figs. 1–7 were performed in triplicate or quadruplicate. All results are expressed as mean ± SEM.

Table 4. Number of motor neurons used to quantify signal intensity in immunostained tissues

Protein	Tissue origin	Motor neuron counts		
		CNIII	CNXII	cSC
Gucy1a3	Wild-type mouse	134	145	137
	SOD1^{G93A} mouse	153	154	67
	ND Control patient	104	96	64
	ALS patient	97	104	64
Parvalbumin	Wild-type mouse	97	51	57
	SOD1^{G93A} mouse	90	47	60
	ND Control patient	100	80	78
	ALS patient	70	63	50
Peripherin	Wild-type mouse	80	83	60
	SOD1^{G93A} mouse	108	116	88
	ND Control patient	92	51	59
	ALS patient	42	52	34
Dynein	Wild-type mouse	91	124	77
	SOD1^{G93A} mouse	115	75	65
	ND Control patient	58	64	37
	ALS patient	61	54	45
Gabra1	Wild-type mouse	112	64	136
	SOD1^{G93A} mouse	48	24	79
	ND Control patient	90	68	63
	ALS patient	92	74	82
Gabra2	Wild-type mouse	65	51	138
	SOD1^{G93A} mouse	43	23	102
	ND Control patient	102	103	126
	ALS patient	125	204	146

RESULTS

Our previous work in the normal rat identified differential gene expression between resistant and vulnerable motor neurons, which may in part underlie their differential susceptibility to disease (Hedlund et al., 2010). In the present work we aimed to understand the regulation of the resulting proteins in health and ALS and across species, utilizing symptomatic fALS mice, end-stage ALS patient tissues and control patient tissues. We selected six genes that show preferential expression either in resistant oculomotor or in vulnerable hypoglossal and spinal motor neurons in the normal rat (Hedlund et al., 2010), including Gucy1a3, parvalbumin, Gabra1, Gabra2, peripherin and dynein. We analyzed the resulting protein levels within resistant oculomotor and vulnerable hypoglossal and spinal motor neuron somas. A summary of the expression data presented below in the results section and the known biological functions of the proteins can be found in Tables 1 and 5, respectively.

Gucy1a3 and parvalbumin are regulated in ALS in human and mouse

Our analysis of protein expression within resistant and vulnerable motor neuron somas in health and ALS, using immunofluorescent staining and immunohistochemistry, was initiated by measuring the levels of Gucy1a3 and parvalbumin. Gucy1a3, which functions as the main receptor for nitric oxide (Zabel et al., 1998) and thus could be implicated in modulating Fas ligand activation (Hedlund et al., 2010), showed the highest relative fluorescent intensity in oculomotor motor neurons in wild-type mice (Fig. 1A–D, $F(2, 413) = 26.72$, $P < 0.0001$). In SOD1^{G93A} mice Gucy1a3 was instead present at comparable levels in all motor neuron nuclei measured (Fig. 1E–H, $F(2, 371) = 1.179$, $P = 0.3086$). There was a significant down-regulation of Gucy1a3 in all motor neuron groups in SOD1^{G93A} mice compared to wild-type littermates. Specifically, fluorescence intensity levels decreased from 1.07 ± 0.04 to 0.63 ± 0.02 in oculomotor neurons, from 0.82 ± 0.03 to 0.65 ± 0.02 in hypoglossal and from 0.82 ± 0.02 to 0.54 ± 0.03 in spinal motor neurons (Fig. 1Q, $F(1, 784) = 166.8$, $P < 0.0001$). The level of the calcium-binding protein parvalbumin was the highest in oculomotor motor neurons (1.04 ± 0.06 relative intensity) in control mice. The parvalbumin levels were also high in spinal motor neurons (0.73 ± 0.03), while almost absent in hypoglossal motor neurons (0.17 ± 0.03), consistent with previous studies (Laslo et al., 2000) (Fig. 1I–L, $F(2, 202) = 69.89$, $P < 0.0001$). In the SOD1^{G93A} mice, the level of parvalbumin was now instead the highest in spinal motor neurons (1.37 ± 0.08) (Fig. 1M–P, $F(2, 194) = 64.53$, $P < 0.0001$), due to a significant decrease in relative intensity from 1.04 ± 0.06 to 0.63 ± 0.04 in oculomotor neurons (Fig. 1Q, $F(1, 396) = 9.883$, $P < 0.0001$). To control for unspecific antibody labeling we omitted either the primary antibody or the secondary antibody from the staining protocol. This analysis confirmed that all stainings conducted for this study were specific. Representative images of the negative control

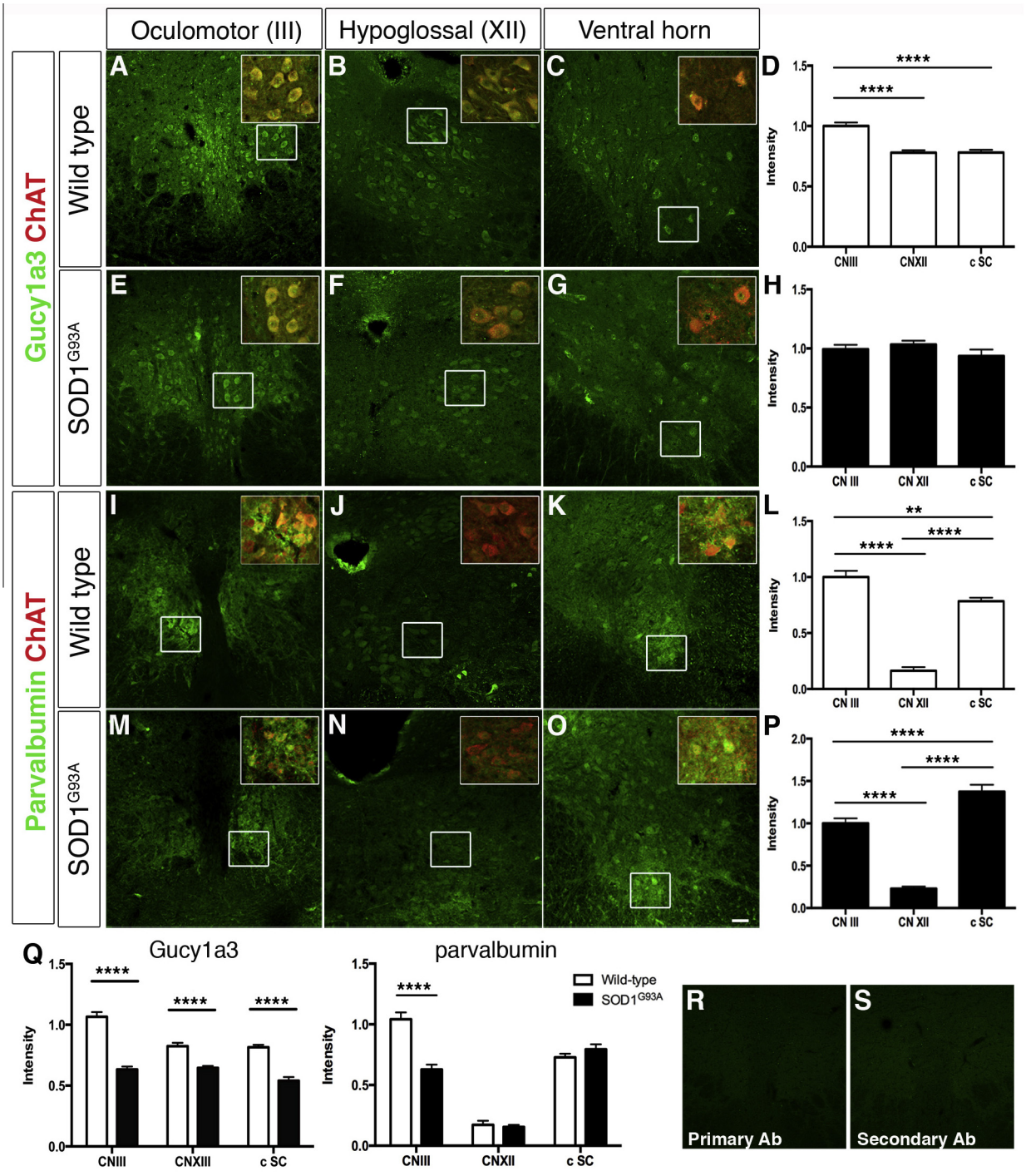

Fig. 1. Gucy1a3 and parvalbumin show differential motor neuron expression and are regulated during motor neuron disease in SOD1^{G93A} fALS mice. Immunofluorescence was used to analyze protein expression patterns and levels in wild-type and SOD1^{G93A} mice at P112. Gucy1a3 (A–D) was preferential to oculomotor motor neurons ($P < 0.0001$, $n = 4$, ANOVA) in wild-type mice. In symptomatic SOD1^{G93A} fALS mice, Gucy1a3 protein levels were comparable in all motor neuron pools measured (E–H, $P = 0.3086$, $n = 4$, ANOVA). All motor neuron groups showed a significant down-regulation of Gucy1a3 with disease (Q, $P < 0.0001$, $n = 4 + 4$, 2-way ANOVA). Parvalbumin levels were the highest in oculomotor neurons in control mice, followed by spinal motor neurons (I–L; $P < 0.0001$, $n = 4$, ANOVA). However, in the SOD1^{G93A} mice parvalbumin levels were instead the highest in spinal motor neurons, followed by oculomotor neurons (M–P; $P < 0.0001$, $n = 4$, ANOVA), due to a significant drop in parvalbumin intensity level in oculomotor motor neurons compared to wild-type (Q, $P < 0.0001$, $n = 4 + 4$, 2-way ANOVA). Negative control stainings, to control for unspecific labeling by antibodies were done by omitting either the primary or secondary antibodies. Staining against parvalbumin using primary antibody only (R) or secondary antibody only (S) did not result in any unspecific staining. Scale bar = 50 μm in O, applicable to A–O.

Table 5. Summary of candidate protein analysis across species in health and ALS

Protein	Motor neurons with highest protein level			Changes in protein levels in disease	Relevant figures
	Control mouse	Control human patient	End stage ALS human patient	Symptomatic fALS mouse	
Gucy1a3	CNIII	CNIII	All motor neurons	Yes	Figs. 1 and 3
Parvalbumin	CNIII	SC	CNIII	Yes	Figs. 1–3
Gabra1	CNIII	CNIII	CNIII	Yes	Figs. 4 and 5
Gabra2	SC	SC	SC	No	Figs. 4 and 5
Peripherin	SC	CNXII and SC	CNXII and SC	Yes	Figs. 6 and 7
Dynein	SC	CNXII and SC	All motor neurons	Yes	Figs. 6 and 7

CNIII = oculomotor nucleus, CNXII = hypoglossal nucleus, SC = spinal cord.

stainings are shown for parvalbumin in midbrain tissue, including CNIII, using either primary antibody only (Fig. 1R) or secondary antibody only (Fig. 1S). Importantly, parvalbumin levels differed greatly among motor neurons within CNIII (Fig. 2A–C, J, standard deviation (SD) = 0.54) and CNIV in control animals (Fig. 2D–F) and in symptomatic $SOD1^{G93A}$ mice (Fig. 2K, SD = 0.56). Thus, while most motor neurons in these resistant nuclei expressed parvalbumin, some appeared almost devoid of this protein. Spinal cord motor neurons showed relatively homogenous parvalbumin levels in wild-type animals (Fig. 2G–J, SD = 0.24). However, in disease expression levels varied greatly between individual spinal motor neurons (Fig. 2K, SD = 0.63) with a 2.6-fold increase in standard deviation compared to wild-type when considering relative intensity levels between cells.

To investigate if these two proteins could potentially play a role in motor neuron resistance and vulnerability in man we performed an analysis in postmortem brain and spinal cord tissues from ND controls and ALS patients. Gucy1a3 protein levels were the highest in oculomotor neurons (1 ± 0.03 relative intensity), followed by hypoglossal motor neurons (0.89 ± 0.04) and lowest in spinal motor neurons (0.74 ± 0.05) in control tissues (Fig. 3A–E, $F(2, 261) = 12.73$, $P < 0.0001$). Thus, the higher expression in oculomotor neurons appears conserved between mouse and man. In end-stage ALS patients, Gucy1a3 was still present in oculomotor neurons, but the levels were not significantly different from motor neurons in CNXII and the spinal cord (Fig. 3F–I, $F(2, 262) = 3{,}241$, $P = 0.0407$). This is similar to the pattern seen in the symptomatic $SOD1^{G93A}$ mouse.

Parvalbumin levels were the highest in spinal motor neurons (1.19 ± 0.05 relative intensity) in control patient tissues, followed by oculomotor neurons (1.00 ± 0.03). The level of parvalbumin in hypoglossal motor neurons (0.64 ± 0.03) was significantly lower compared to both oculomotor and spinal motor neurons (Fig. 3J–M, $F(2, 255) = 52.51$, $P < 0.0001$), consistent with the mouse. In ALS patients, parvalbumin levels were significantly higher in oculomotor motor neurons (1.00 ± 0.06) compared to spinal (0.72 ± 0.06) and hypoglossal (0.68 ± 0.05) motor neurons (Fig. 3N–Q, $F(2, 180) = 11.27$, $P < 0.0001$).

Gabra1 and Gabra2 show opposing motor neuron expression patterns

It has been proposed that different levels of excitability can underlie some of the differences in motor neuron vulnerability in ALS. The $SOD1^{G93A}$ mice show motor neuron hyperexcitability early in life (van Zundert et al., 2008) and insufficient synaptic inhibition (Lorenzo et al., 2006; Chang and Martin, 2011), which can be modulated through glycine and $GABA_A$ receptor expression. We therefore investigated the expression pattern of Gabra1 and (Gabra2) in mouse and man and in health and ALS. Our analysis showed that Gabra1 was preferentially expressed in oculomotor motor neurons in wild-type (Fig. 4A–D, $F(2, 309) = 97.18$, $P < 0.0001$) and $SOD1^{G93A}$ mice (Fig. 4E–H, $F(2, 148) = 62.86$, $P < 0.0001$).

In the ALS mice, Gabra1 protein levels were increased compared to wild-type, from a relative intensity of 1.00 ± 0.03 to 1.47 ± 0.07 in oculomotor motor neurons and from 0.64 ± 0.02 to 0.90 ± 0.03 in spinal motor neurons (Fig. 4Q, $F(1, 469) = 55.69$, $P < 0.0001$). Gabra2 showed the opposite pattern to Gabra1, with preferential localization in spinal motor neurons (1.74 ± 0.07 relative intensity) and lower levels in hypoglossal (1.11 ± 0.09) and oculomotor (1.00 ± 0.07) motor neurons in wild-type mice (Fig. 4I–L, $F(2, 251) = 40.75$, $P < 0.0001$). Gabra2 was also present at the highest level in spinal motor neurons (1.92 ± 0.04) in $SOD1^{G93A}$ mice (Fig. 4M–P, $F(2, 165) = 89.46$, $P < 0.0001$), at levels comparable to wild-type (Fig. 4Q, $F(1, 415) = 2.141$, $P = 0.1442$).

Analysis of the signal intensity of Gabra1 staining in human tissues showed that Gabra1 was preferential to oculomotor motor neurons (1.00 ± 0.02 relative intensity) compared to hypoglossal (0.66 ± 0.05) and spinal (0.60 ± 0.06) in control patients (Fig. 5A–D, $F(2, 218) = 24.14$, $P < 0.0001$). The relatively high level of Gabra1 in oculomotor neurons was maintained in ALS patient tissues (Fig. 5E–H, $F(2, 245) = 32.74$, $P < 0.0001$). These data are consistent with our findings in mouse. Gabra2 showed predominant expression in spinal motor neurons in control patients (Fig. 5I–L, $F(2, 328) = 16.29$, $P < 0.0001$) and ALS patients (Fig. 5M–P, $F(2, 472) = 8.361$, $P = 0.0003$). Collectively, our data showed that $GABA_A$ receptor

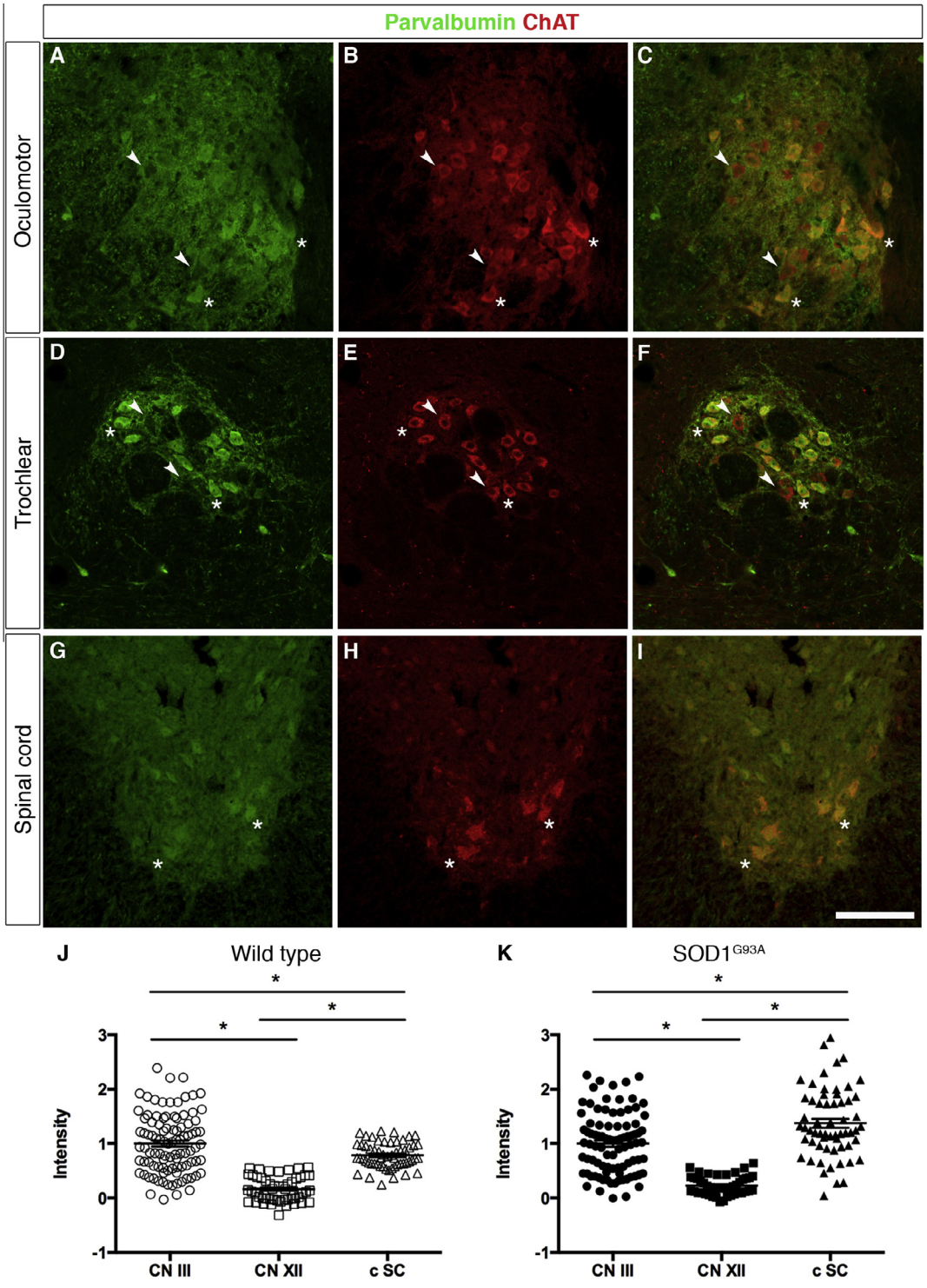

Fig. 2. Levels of parvalbumin differ greatly between individual motor neurons within an anatomical motor nucleus. Confocal analysis showed that parvalbumin was present at different levels in ChAT^{+} motor neurons within the oculomotor nucleus (A–C) and the trochlear nucleus (D–F) in wild-type mice (J, standard deviation (SD) = 0.54, n = 97 motor neurons) and in SOD1^{G93A} mice (K, SD = 0.56, n = 90 motor neurons). Parvalbumin levels were relatively uniform in spinal motor neurons in wild-type mice (G–J, SD = 0.24, n = 57 motor neurons), while the intensity varied greatly in SOD1^{G93A} mice (K, SD = 0.63, n = 60 motor neurons). Arrows indicate ChAT^{+} motor neurons that appear to be devoid of parvalbumin, while asterisks exemplify motor neurons that have high levels of parvalbumin. Scale bar = 100 μm in I, applicable to A–I.

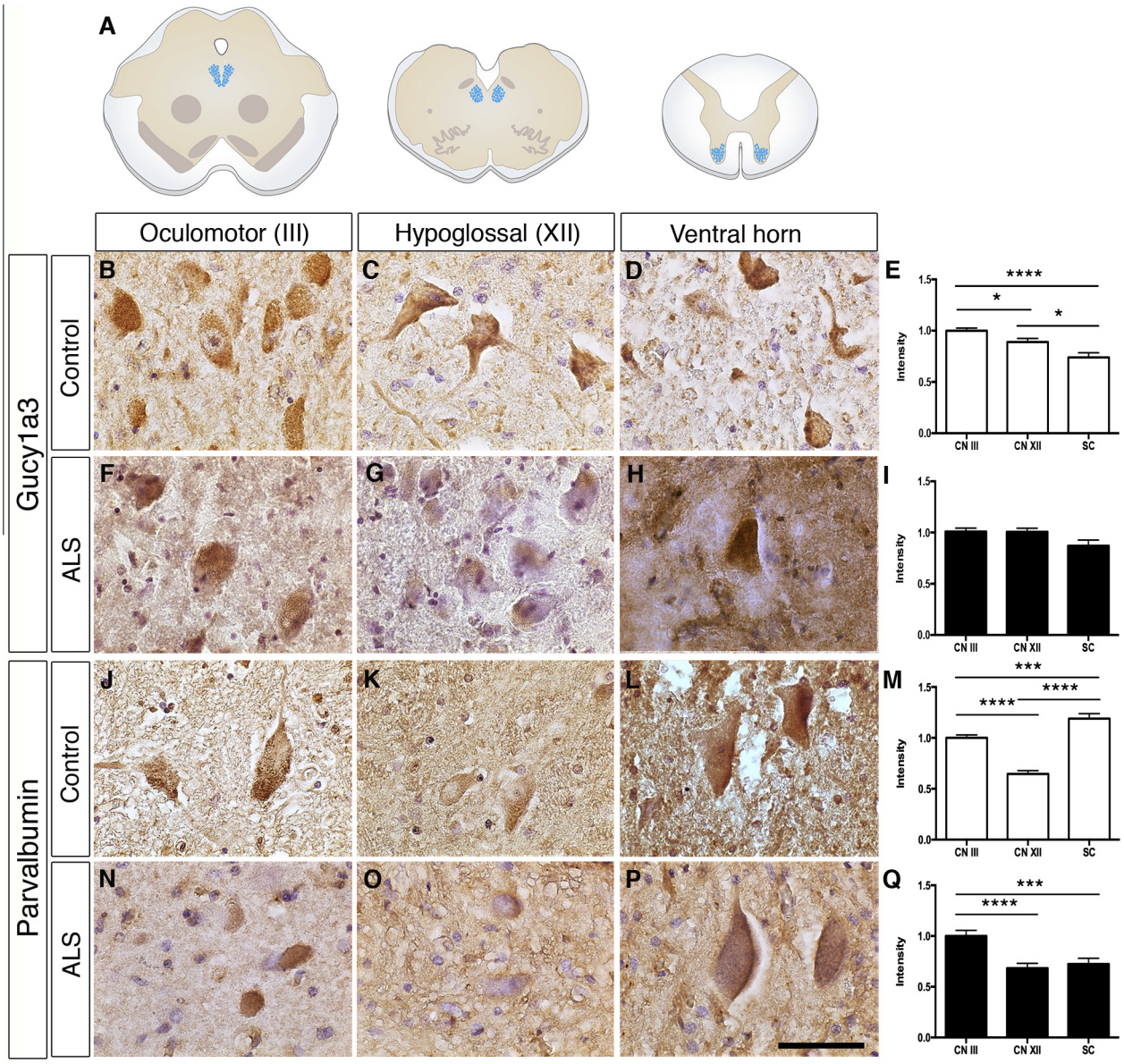

Fig. 3. Gucy1a3 and parvalbumin expression in non-demented control and end-stage ALS patient tissues. Motor neurons in the resistant oculomotor nucleus and the vulnerable hypoglossal nucleus and ventral horn of spinal cord (shown in schematic A) in non-demented and ALS patient tissues were analyzed for expression levels of proteins with predominant expression in oculomotor motor neurons in mouse. Gucy1a3 showed predominant localization to oculomotor motor neurons in control patients (B–E, $P < 0.0001$, $n = 4$, ANOVA), while in ALS patients the level of Gucy1a3 was similar in all motor neuron groups (F-I, $P = 0.0407$, $n = 4$, ANOVA). Parvalbumin was preferentially expressed in oculomotor and spinal motor neurons compared to hypoglossal motor neurons in control, with the highest level in spinal motor neurons (J–M, $P < 0.0001$, $n = 4$, ANOVA). In end-stage ALS patient tissue the level was the highest in oculomotor motor neurons (N–Q, $P < 0.0001$, $n = 4$, ANOVA). Scale bar = 20 μm in P, applies to B–P.

distribution differed between resistant and vulnerable motor neurons in control mice and control patients. These differences were maintained after the onset of disease in $SOD1^{G93A}$ mice and in end-stage ALS patients.

Peripherin and dynein are preferential to vulnerable motor neurons in human and mouse and are regulated in disease

Finally, we examined the dynamics of peripherin and dynein protein levels in health and ALS. Peripherin, which is an intermediate neurofilament, was investigated due to its previously shown associations with ALS (He and Hays, 2004; Leung et al., 2004; Xiao et al., 2008) and its preferential expression in vulnerable spinal motor neurons in the normal rat (Hedlund et al., 2010). Quantification of fluorescent intensity within motor neuron somas showed that peripherin was predominantly expressed in spinal motor neurons in wild-type (Fig. 6A–D, $F(2, 220) = 32.71$ $P < 0.0001$) and $SOD1^{G93A}$ mice (Fig. 6E–H, $F(2, 333) = 103.9$ $P < 0.0001$). The relative level of peripherin increased specifically in spinal motor neurons from 1.18 ± 0.06 to 1.41 ± 0.06 in the $SOD1^{G93A}$ mice, while it decreased in oculomotor (from

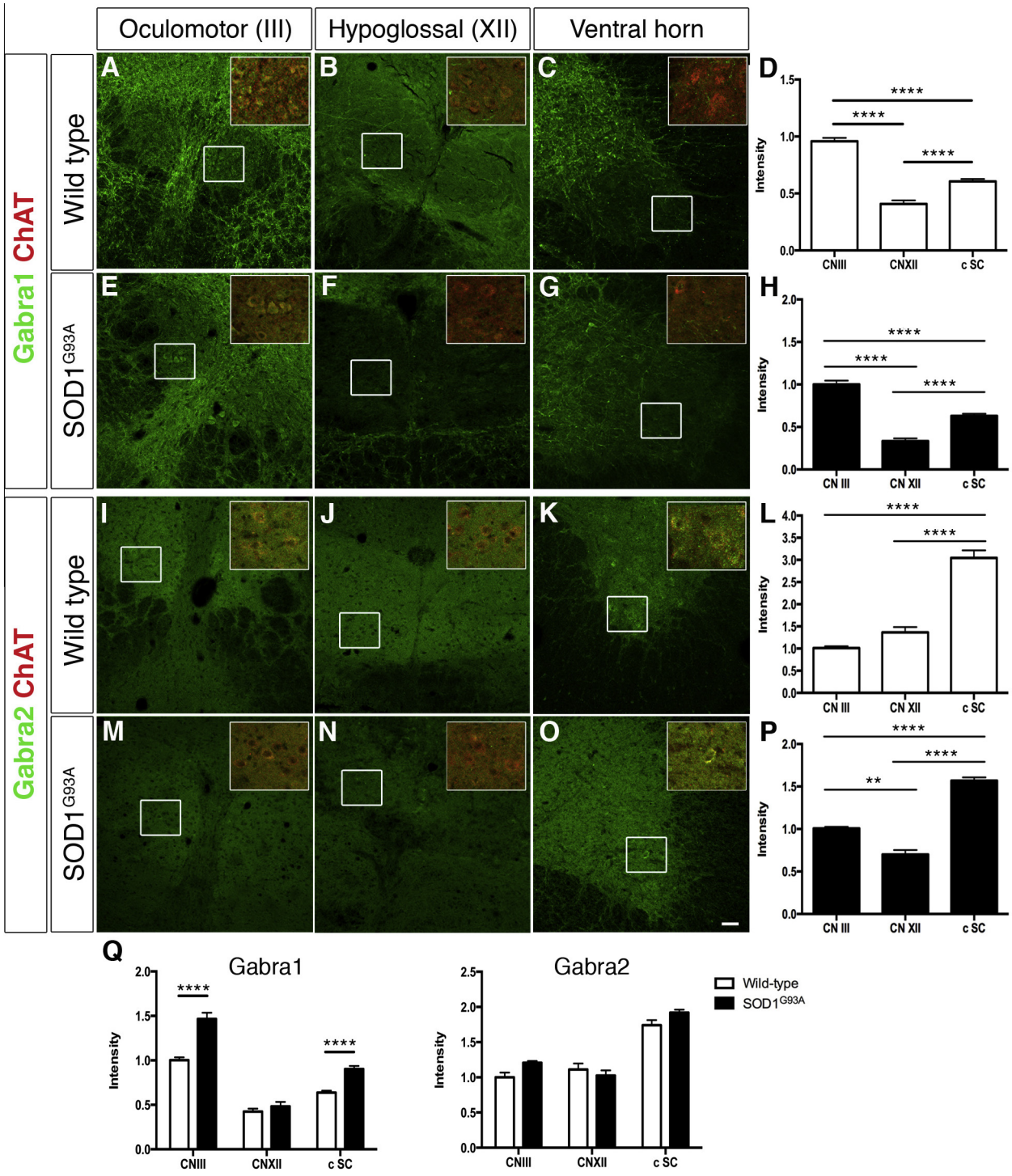

Fig. 4. Gabra1 and Gabra2 show opposing expression in resistant and vulnerable motor neurons in mouse. Immunofluorescent analysis and quantification of relative intensity levels within motor neurons in wild-type mice showed that Gabra1 was preferentially expressed in oculomotor motor neurons. Hypoglossal motor neurons showed the lowest Gabra 1 protein level (A-D, $P < 0.0001$, $n = 5$, ANOVA). In the SOD1^{G93A} fALS mice, Gabra1 continued to be preferentially expressed in oculomotor motor neurons (E–H, $P < 0.0001$, $n = 3$, ANOVA). The levels of Gabra1 remained relatively high in spinal motor neurons than in hypoglossal motor neurons in the SOD1^{G93A} mice (H, $P < 0.0001$, $n = 3$, ANOVA). Furthermore, there was a relative increase in expression in oculomotor and spinal motor neurons in ALS mice compared to wild-type mice (Q, $P < 0.0001$, $n = 5 + 3$, 2-way ANOVA). Gabra2 was preferential to spinal motor neurons in wild-type mice (I–L, $P < 0.0001$, $n = 4$, ANOVA). Gabra2 was present at the highest level in spinal motor neurons also in SOD1^{G93A} mice. Furthermore, in the ALS mice, Gabra2 showed a relatively high expression in oculomotor motor neurons than in hypoglossal motor neurons (P, $P < 0.0001$, $n = 3$, ANOVA). Disease did not induce significant changes in Gabra2 levels for the motor neuron groups analyzed (Q, $P = 0.1442$, $n = 4 + 3$, 2-way ANOVA). Scale bar = 50 μm in O, applicable to A–O.

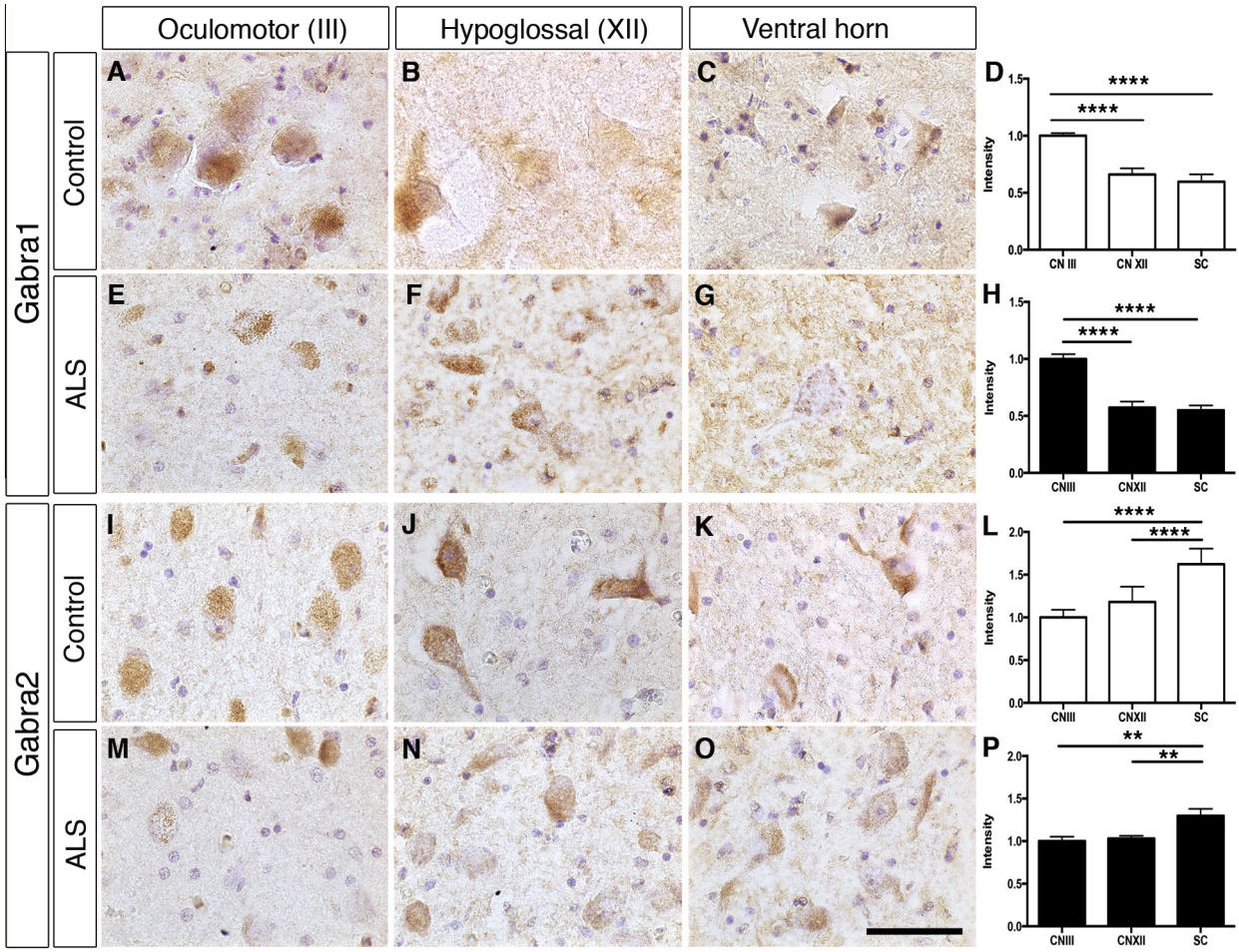

Fig. 5. Gabra1 and Gabra2 show distinct motor neuron expression patterns in control and ALS patient tissues. Quantification of immunohistochemical signal intensity revealed that Gabra1 was preferentially expressed in oculomotor motor neurons in control patient tissues (A–D, $P < 0.0001$, $n = 3$, ANOVA) and in end-stage ALS patient tissues (E–H, $P < 0.0001$, $n = 3$, ANOVA). Gabra2 was present at the highest level in spinal motor neurons in non-demented patient control tissue (I–L, $P < 0.0001$, $n = 3$, ANOVA). In end-stage ALS patient tissue, Gabra2 still remained the highest in spinal motor neurons. However, the differences between spinal motor neurons and the other motor neuron groups was reduced (M–P, $P = 0.0003$, $n = 3$, ANOVA). Scale bar = 20 μm in O, applies to A–O.

1.01 ± 0.06 to 0.63 ± 0.02) and hypoglossal motor neurons (from 0.97 ± 0.04 to 0.72 ± 0.04) with disease (Fig. 6Q, $F(1, 529) = 12.51$, $P = 0.0004$).

The motor protein dynein is important for retrograde transport, which is disrupted in ALS (Tanaka et al., 2012) thereby making its regulation of interest. Dynein levels were the highest in spinal motor neurons (2.43 ± 0.10 relative intensity), but were also significantly higher in hypoglossal (1.25 ± 0.06) than oculomotor (1.00 ± 0.05) motor neurons in wild-type (Fig. 6I–L, $F(2, 289) = 116.7$, $P < 0.0001$). $SOD1^{G93A}$ mice showed the same pattern of relative protein levels (Fig. 6M–P, $F(2, 252) = 68.57$, $P < 0.0001$), but the levels were significantly decreased in all motor neuron nuclei compared to wild-type mice (Fig. 6Q, $F(1, 541) = 423.1$, $P < 0.0001$).

Analysis of human tissues showed that peripherin was preferentially present in hypoglossal (1.72 ± 0.08) and spinal motor neurons (1.59 ± 0.09) compared to oculomotor motor neurons (1.00 ± 0.04) in control patients (Fig. 7A–D, $F(2, 200) = 39.84$, $P < 0.0001$). This pattern was maintained in ALS patients (Fig. 7E–H, $F(2, 125) = 17.24$, $P < 0.0001$). The higher level of peripherin within spinal motor neurons than oculomotor motor neurons appears consistent between man and mouse, while the relatively high levels in hypoglossal motor neurons appears specific to man. Dynein was also preferential to hypoglossal (1.25 ± 0.06) and spinal (1.38 ± 0.07) motor neurons compared to oculomotor motor neurons (1.00 ± 0.05) in control patients (Fig. 7I–L, $F(2, 127) = 11.11$, $P < 0.0001$), similar to mouse. In end-stage ALS patients, dynein expression was comparable in all motor neuron groups (Fig. 7M–P, $F(2, 157) = 0.3510$, $P = 0.7046$), through an apparent decrease of protein levels (Fig. 7I–K versus M–O), similarly to symptomatic fALS mice. Collectively, our data show that dynein and peripherin are present at higher levels in vulnerable than resistant motor neurons in both man and mouse. It is also clear that there is modulation of these proteins in disease, which would result in dysregulation of retrograde transport.

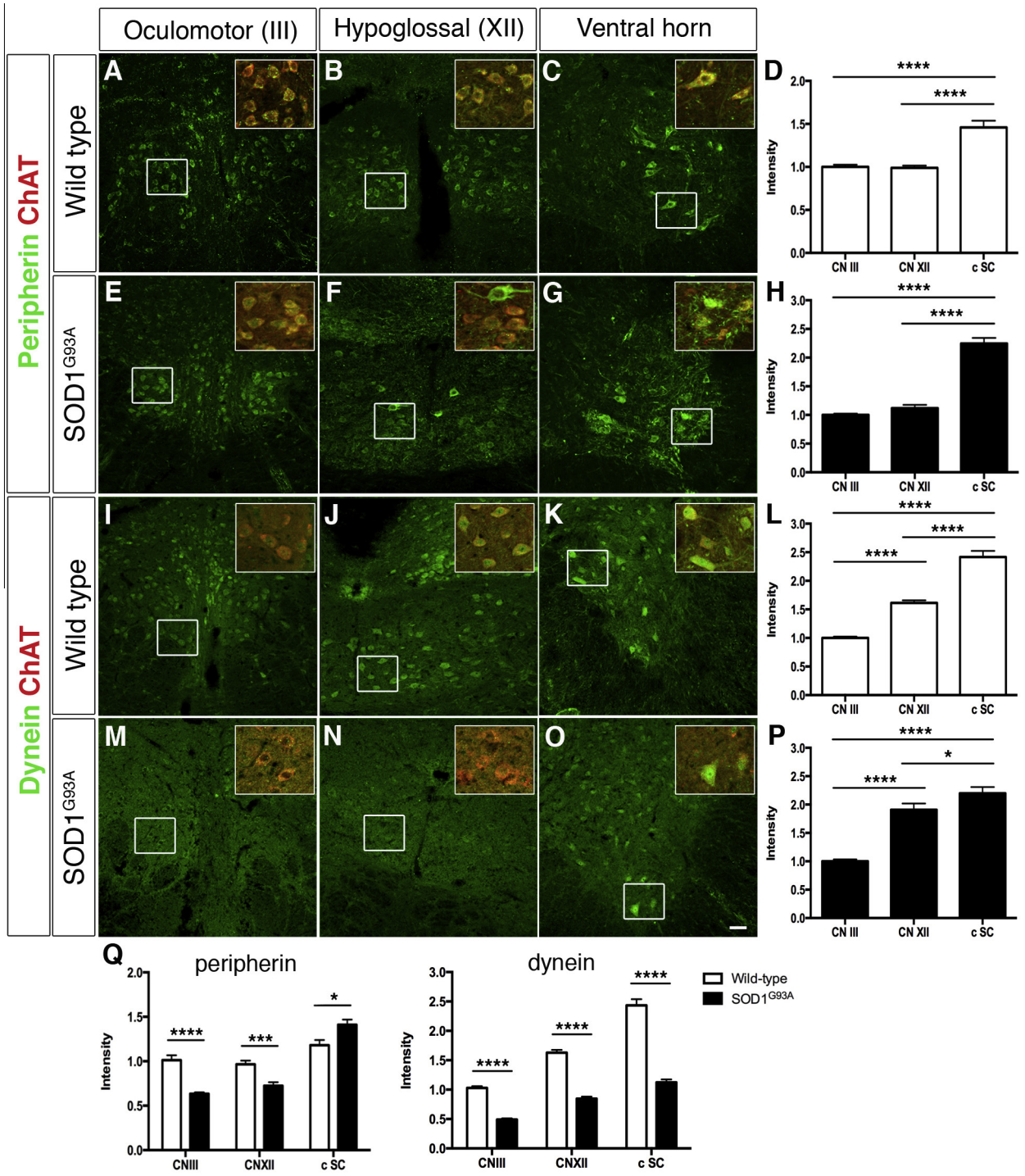

Fig. 6. Peripherin and dynein are preferentially expressed in vulnerable motor neurons in wild-type and SOD1^{G93A} fALS mice. Peripherin protein levels were significantly higher in motor neurons of the spinal cord than those in the oculomotor and hypoglossal nucleus of wild-type mice (A–D, $P < 0.0001$, $n = 3$, ANOVA) and SOD1^{G93A} mice (E–H, $P < 0001$, $n = 4$, ANOVA. Peripherin was specifically increased in spinal motor neurons in the ALS mice, while the levels decreased in oculomotor and hypoglossal motor neurons with disease (Q, $P = 0.0004$, $n = 3 + 4$, 2-way ANOVA). Dynein levels were the highest in spinal motor neurons followed by hypoglossal motor neurons in both control mice (I–L, $P < 0.0001$, $n = 4$, ANOVA) and symptomatic ALS mice (M–P, $P < 0.0001$, $n = 4$, ANOVA). Dynein was decreased in all motor neuron nuclei in the SOD1^{G93A} mice compared to wild-type mice (Q, $P < 0.0001$, $n = 4 + 4$, 2-way ANOVA). Scale bar = 50 μm in O, applicable to A–O.

DISCUSSION

Neurodegenerative diseases are characterized by a selective degeneration of specific neuronal populations. Identification of mechanisms of vulnerability and resistance among neurons with similar properties that respond differentially to disease-inducing mutations could lead to future therapies. Motor neurons that innervate

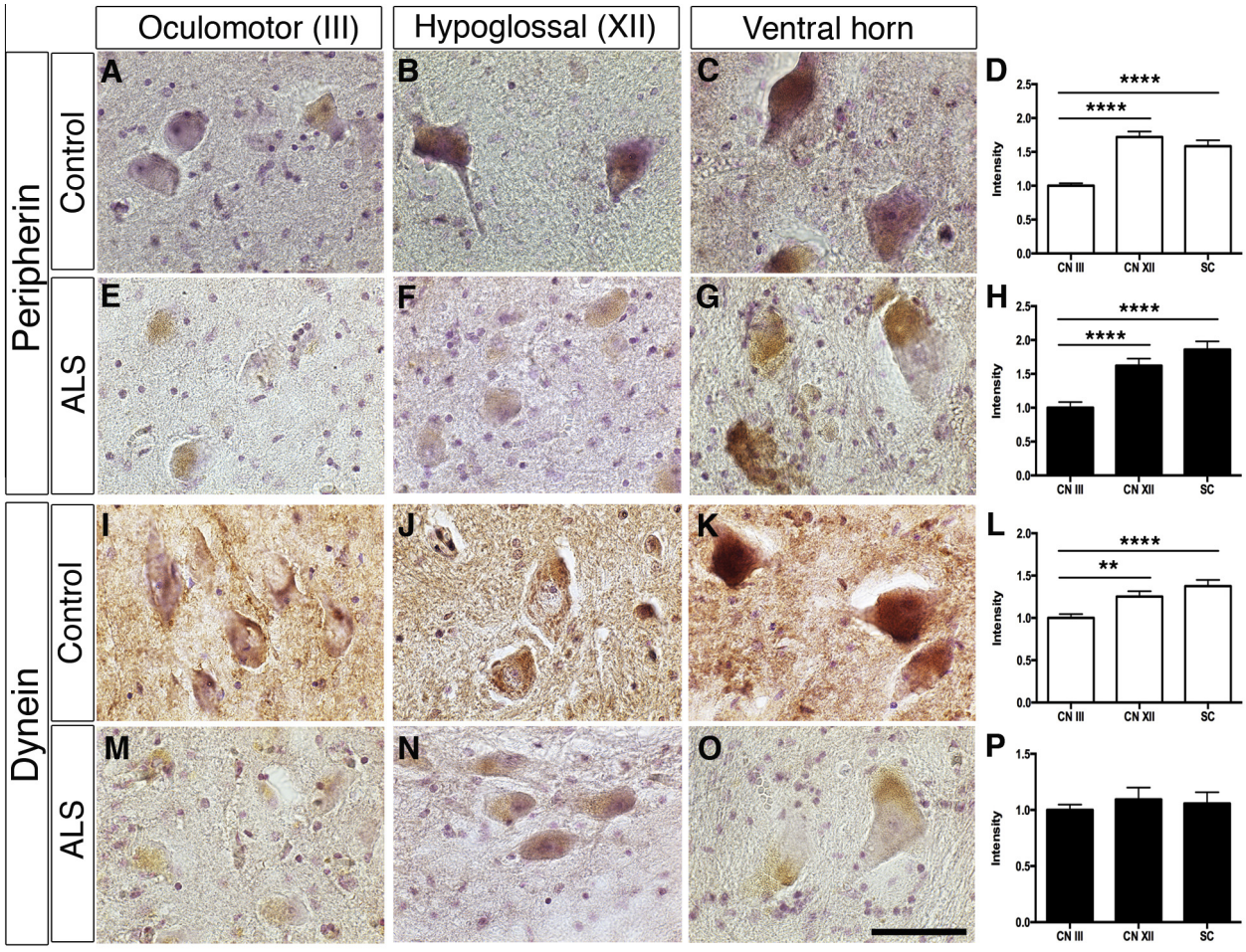

Fig. 7. Peripherin and dynein show predominant expression in vulnerable hypoglossal and spinal motor neurons in human patient tissues. Peripherin was preferential to hypoglossal and spinal motor neurons compared to oculomotor motor neurons in non-demented control patients (A–D, $P < 0.0001$, $n = 3$, ANOVA). Peripherin remained restricted to spinal and hypoglossal motor neurons in end-stage ALS patient tissues (E–H, $P < 0.0001$, $n = 3$, ANOVA). Dynein was also preferential to spinal and hypoglossal motor neurons in control patient tissues (I–L, $P < 0.0001$, $n = 3$, ANOVA), while in ALS patients the levels were comparable in all motor neurons groups (M–P, $P = 0.7046$, $n = 4$, ANOVA). Scale bar = 20 μm in O, applies to A–O.

voluntary muscles degenerate in the lethal disease ALS. However, oculomotor motor neurons that regulate eye movement are for unknown reasons resistant to degeneration. In this report we have identified a protein signature for oculomotor motor neurons in health and in ALS with the aim of understanding motor neuron resistance.

We initially considered Gucy1a3 to be a potential candidate for explaining motor neuron resistance, as it is preferential to oculomotor motor neurons in wild-type rats (Hedlund et al., 2010) and mice. Gucy1a3 could limit unbound NO in the cell and consequently lower levels of Fas activation, which is detrimental to the cells (Hedlund et al., 2010). However, Gucy1a3 was evenly distributed between resistant oculomotor and vulnerable hypoglossal and spinal motor neurons in symptomatic $SOD1^{G93A}$ mice and ALS patients, thus rendering it an unlikely candidate to explain oculomotor resistance.

Parvalbumin has been implicated in oculomotor motor neuron resistance and its over-expression can increase the resistance of motor neurons to Ca^{2+}-currents, induced through nerve injury (Dekkers et al., 2004) or excitotoxic challenge (Van Den Bosch et al., 2002). However, several of our findings argue against parvalbumin being a major factor in oculomotor resistance. As shown here, resistant oculomotor and vulnerable spinal motor neurons contained relatively similar levels of parvalbumin in both mouse and man. Furthermore, in symptomatic $SOD1^{G93A}$ mice, parvalbumin levels dropped significantly in oculomotor motor neurons, while remaining unchanged in spinal motor neurons. Finally, we could show that levels of parvalbumin differed greatly between individual motor neurons, with some oculomotor motor neurons lacking parvalbumin in both health and ALS despite their resistant phenotype.

Inhibitory synaptic transmission, mediated by GABA and glycine neurotransmission, appears to differ between oculomotor and hypoglossal motor neurons and may in part underlie their differential vulnerability (Lorenzo et al., 2006). Our study of Gabra1 and Gabra2 expression complements previous analyses in control animals (Lorenzo et al., 2006; Brockington et al., 2013) and

control patients (Brockington et al., 2013), showing that Gabra1 was preferentially present in oculomotor motor neurons. In addition we also show that Gabra1 remains preferential to oculomotor motor neurons in symptomatic SOD1^{G93A} mice and in end-stage ALS patients. This could indicate Gabra1 as a candidate for oculomotor resistance. Conversely, Gabra2 was preferential to spinal motor neurons in man and mouse in health and in ALS. However, the relative difference in Gabra2 levels between oculomotor and spinal motor neurons in man appeared smaller in ALS patient motor neurons (1.3-fold) than in control patients (1.6-fold). This could either indicate a regulation of Gabra2 levels or loss of spinal motor neurons with higher levels of Gabra2. Finally, our data on Gabra1 and Gabra2 indicate that differences in inhibitory synaptic transmission between resistant oculomotor and vulnerable motor neurons are largely maintained even at end-stage of disease.

From our findings it appears that oculomotor motor neurons in mouse and man have lower levels of the motor protein dynein and the intermediate neurofilament peripherin. This might simply reflect a lesser need for retrograde transport due to a smaller cell body size, shorter axon and lower energy dependence. Additionally, it might render oculomotor motor neurons less vulnerable to changes in retrograde transport, which are known to occur in ALS (Collard et al., 1995) and which we indirectly document here. Indeed, dysregulation in either the dynein–dynactin complex (LaMonte et al., 2002; Hafezparast et al., 2003) or peripherin (Beaulieu et al., 1999) causes spinal motor neuron degeneration in mice, presumably through defective axonal transport (LaMonte et al., 2002; Hafezparast et al., 2003; Millecamps et al., 2006). Furthermore, sALS patient spinal motor neurons show decreased levels of dynactin (Jiang et al., 2007). Our human tissue analyses showed that dynein was preferential to hypoglossal and spinal motor neurons in control patient tissues, while in ALS patients dynein was present at similar levels in all motor neuron groups. These data could either reflect a decrease of dynein in vulnerable motor neurons or a loss of the motor neurons that expressed high levels of dynein to begin with. Based on these data it is compelling to infer that motor neurons that are less dependent on retrograde transport normally might do better in disease when there is a dramatic decrease in dynein, as seen here in the SOD1^{G93A} mouse. However, impaired dynein function actually appears beneficial in the mutant SOD1 fALS mice (Kieran et al., 2005). This indicates that the decrease in dynein within SOD1^{G93A} motor neurons during disease progression could in part be beneficial and reflect a protective need to decrease axonal transport, but this remains to be addressed. Peripherin, on the other hand, remained preferential to motor neurons in the spinal cord also in ALS patient tissue. However, our data indicate that normal physiological differences in peripherin levels *per se* are not necessarily a factor of vulnerability. In fact, the increase in peripherin levels in spinal motor neurons in the SOD1^{G93A} mice and the persistence of peripherin in spinal motor neurons remaining in end-stage patients could instead reflect regenerative responses in degenerating axons. Such a regenerative response is indicated through the presence of peripherin^{+} ChAT-negative neurons in the CNXII and spinal cord in SOD1^{G93A} mice, and will be subjected to further investigation.

CONCLUSION

We have identified a protein signature for oculomotor motor neurons in health and in ALS, which could in part explain their preservation in disease both in man and mouse. The relative conservation of signals across species infers that transgenic SOD1^{G93A} mice could be used to predict mechanisms of motor neuron susceptibility in man.

Acknowledgments—We want to thank S Cullheim for many helpful discussions and for critically reading this manuscript. We thank A Bergstrand for excellent help with sectioning and histology. This work was funded by grants from the Söderberg Foundation (M245/11) (E.H.), the Birgit Backmark Donation for ALS research (E.H.), the Thierry Latran Foundation (S.C.; E.H.), the Swedish Medical Research Council (2011–2651) (E.H.), the Åhlen's Foundation (mA5/h12, mA9/11) (E.H.) and the Swedish Brain Foundation (FO2012-0055) (E.H). Human post mortem tissues were kindly received from the Netherlands Brain Bank (NBB) and the National Disease Research Interchange (NDRI). The authors thank Mattias Karlen for his excellent work generating the schematic of human brain sections in Fig. 3 for this paper.

REFERENCES

Al-Chalabi A, Jones A, Troakes C, King A, Al-Sarraj S, et al. (2012) The genetics and neuropathology of amyotrophic lateral sclerosis. Acta Neuropathol 124:339–352.

Beaulieu JM, Nguyen MD, Julien JP (1999) Late onset of motor neurons in mice overexpressing wild-type peripherin. J Cell Biol 147:531–544.

Boillee S, Yamanaka K, Lobsiger CS, Copeland NG, Jenkins NA, et al. (2006) Onset and progression in inherited ALS determined by motor neurons and microglia. Science 312:1389–1392.

Brockington A, Ning K, Heath PR, Wood E, Kirby J, et al. (2013) Unravelling the enigma of selective vulnerability in neurodegeneration: motor neurons resistant to degeneration in ALS show distinct gene expression characteristics and decreased susceptibility to excitotoxicity. Acta Neuropathol 125:95–109.

Chang Q, Martin LJ (2011) Glycine receptor channels in spinal motoneurons are abnormal in a transgenic mouse model of amyotrophic lateral sclerosis. J Neurosci 31:2815–2827.

Collard JF, Cote F, Julien JP (1995) Defective axonal transport in a transgenic mouse model of amyotrophic lateral sclerosis. Nature 375:61–64.

Das MM, Svendsen CN (2014) Astrocytes show reduced support of motor neurons with aging that is accelerated in a rodent model of ALS. Neurobiol Aging.

Dekkers J, Bayley P, Dick JR, Schwaller B, Berchtold MW, et al. (2004) Over-expression of parvalbumin in transgenic mice rescues motoneurons from injury-induced cell death. Neuroscience 123:459–466.

Fischer LR, Culver DG, Tennant P, Davis AA, Wang M, et al. (2004) Amyotrophic lateral sclerosis is a distal axonopathy: evidence in mice and man. Exp Neurol 185:232–240.

Gizzi M, DiRocco A, Sivak M, Cohen B (1992) Ocular motor function in motor neuron disease. Neurology 42:1037–1046.

Gurney ME (1994) Transgenic-mouse model of amyotrophic lateral sclerosis. N Engl J Med 331:1721–1722.
Haenggeli C, Kato AC (2002) Differential vulnerability of cranial motoneurons in mouse models with motor neuron degeneration. Neurosci Lett 335:39–43.
Hafezparast M, Klocke R, Ruhrberg C, Marquardt A, Ahmad-Annuar A, et al. (2003) Mutations in dynein link motor neuron degeneration to defects in retrograde transport. Science 300:808–812.
He CZ, Hays AP (2004) Expression of peripherin in ubiquinated inclusions of amyotrophic lateral sclerosis. J Neurol Sci 217:47–54.
Hedlund E, Karlsson M, Osborn T, Ludwig W, Isacson O (2010) Global gene expression profiling of somatic motor neuron populations with different vulnerability identify molecules and pathways of degeneration and protection. Brain 133:2313–2330.
Huang C, Tong J, Bi F, Zhou H, Xia XG (2012) Mutant TDP-43 in motor neurons promotes the onset and progression of ALS in rats. J Clin Invest 122:107–118.
Jaarsma D, Teuling E, Haasdijk ED, De Zeeuw CI, Hoogenraad CC (2008) Neuron-specific expression of mutant superoxide dismutase is sufficient to induce amyotrophic lateral sclerosis in transgenic mice. J Neurosci 28:2075–2088.
Jiang YM, Yamamoto M, Tanaka F, Ishigaki S, Katsuno M, et al. (2007) Gene expressions specifically detected in motor neurons (dynactin 1, early growth response 3, acetyl-CoA transporter, death receptor 5, and cyclin C) differentially correlate to pathologic markers in sporadic amyotrophic lateral sclerosis. J Neuropathol Exp Neurol 66:617–627.
Kaplan A, Spiller KJ, Towne C, Kanning KC, Choe GT, et al. (2014) Neuronal matrix metalloproteinase-9 is a determinant of selective neurodegeneration. Neuron 81:333–348.
Kieran D, Hafezparast M, Bohnert S, Dick JR, Martin J, et al. (2005) A mutation in dynein rescues axonal transport defects and extends the life span of ALS mice. J Cell Biol 169:561–567.
Kiskinis E, Sandoe J, Williams LA, Boulting GL, Moccia R, et al. (2014) Pathways disrupted in human ALS motor neurons identified through genetic correction of mutant SOD1. Cell Stem Cell 14:781–795.
Kubota M, Sakakihara Y, Uchiyama Y, Nara A, Nagata T, et al. (2000) New ocular movement detector system as a communication tool in ventilator-assisted Werdnig-Hoffmann disease. Dev Med Child Neurol 42:61–64.
LaMonte BH, Wallace KE, Holloway BA, Shelly SS, Ascano J, et al. (2002) Disruption of dynein/dynactin inhibits axonal transport in motor neurons causing late-onset progressive degeneration. Neuron 34:715–727.
Laslo P, Lipski J, Nicholson LF, Miles GB, Funk GD (2000) Calcium binding proteins in motoneurons at low and high risk for degeneration in ALS. NeuroReport 11:3305–3308.
Leung CL, He CZ, Kaufmann P, Chin SS, Naini A, et al. (2004) A pathogenic peripherin gene mutation in a patient with amyotrophic lateral sclerosis. Brain Pathol 14:290–296.
Lorenzo LE, Barbe A, Portalier P, Fritschy JM, Bras H (2006) Differential expression of GABAA and glycine receptors in ALS-resistant vs. ALS-vulnerable motoneurons: possible implications for selective vulnerability of motoneurons. Eur J Neurosci 23:3161–3170.
Millecamps S, Robertson J, Lariviere R, Mallet J, Julien JP (2006) Defective axonal transport of neurofilament proteins in neurons overexpressing peripherin. J Neurochem 98:926–938.
Nimchinsky EA, Young WG, Yeung G, Shah RA, Gordon JW, et al. (2000) Differential vulnerability of oculomotor, facial, and hypoglossal nuclei in G86R superoxide dismutase transgenic mice. J Comp Neurol 416:112–125.
Saxena S, Cabuy E, Caroni P (2009) A role for motoneuron subtype-selective ER stress in disease manifestations of FALS mice. Nat Neurosci 12:627–636.
Schaefer AM, Sanes JR, Lichtman JW (2005) A compensatory subpopulation of motor neurons in a mouse model of amyotrophic lateral sclerosis. J Comp Neurol 490:209–219.
Shaw CE, Enayat ZE, Powell JF, Anderson VE, Radunovic A, et al. (1997) Familial amyotrophic lateral sclerosis. Molecular pathology of a patient with a SOD1 mutation. Neurology 49:1612–1616.
Tanaka F, Ikenaka K, Yamamoto M, Sobue G (2012) Neuropathology and omics in motor neuron diseases. Neuropathology 32: 458–462.
Tjust AE, Brannstrom T, Pedrosa Domellof F (2012) Unaffected motor endplate occupancy in eye muscles of ALS G93A mouse model. Front Biosci (Schol Ed) 4:1547–1555.
Van Den Bosch L, Schwaller B, Vleminckx V, Meijers B, Stork S, et al. (2002) Protective effect of parvalbumin on excitotoxic motor neuron death. Exp Neurol 174:150–161.
van Zundert B, Peuscher MH, Hynynen M, Chen A, Neve RL, et al. (2008) Neonatal neuronal circuitry shows hyperexcitable disturbance in a mouse model of the adult-onset neurodegenerative disease amyotrophic lateral sclerosis. J Neurosci 28:10864–10874.
Waters JC (2009) Accuracy and precision in quantitative fluorescence microscopy. J Cell Biol 185:1135–1148.
Xiao S, Tjostheim S, Sanelli T, McLean JR, Horne P, et al. (2008) An aggregate-inducing peripherin isoform generated through intron retention is upregulated in amyotrophic lateral sclerosis and associated with disease pathology. J Neurosci 28:1833–1840.
Yamanaka K, Chun SJ, Boillee S, Fujimori-Tonou N, Yamashita H, et al. (2008) Astrocytes as determinants of disease progression in inherited amyotrophic lateral sclerosis. Nat Neurosci 11:251–253.
Zabel U, Weeger M, La M, Schmidt HH (1998) Human soluble guanylate cyclase: functional expression and revised isoenzyme family. Biochem J 335(Pt. 1):51–57.

(Accepted 7 February 2015)
(Available online 16 February 2015)